Journal of Organometallic Chemistry 695 (2010) 2048–2056

Contents lists available at ScienceDirect

Journal of Organometallic Chemistry

journal homepage: www.elsevier.com/locate/jorganchem

Ruthenium (II) polypyridyl complexes based on bipyridine and two novel diimine ligands with carrier-transporting unit: synthesis, photoluminescence and redox properties

Jing Wu, Hong-Yan Li, Ling-Chen Kang, Dong-Ping Li, Qiu-Lei Xu, Yu-Cheng Zhu, Yun-Mei Tao, You-Xuan Zheng*, Jing-Lin Zuo, Xiao-Zeng You

State Key Laboratory of Coordination Chemistry, School of Chemistry and Chemical Engineering, Nanjing University, Nanjing National Laboratory of Microstructures, Nanjing 210093, P.R.China

ARTICLE INFO

Article history:
Received 8 March 2010
Received in revised form
27 April 2010
Accepted 30 April 2010
Available online 6 May 2010

Keywords:
Ruthenium
Diimine ligands
Oxadiazole
Carbazole
Photoluminescence

ABSTRACT

A series of ruthenium (II) complexes, $[Ru(bpy)_2L]X_2$ (**L** = L1, L2; X = Cl^-, PF_6^-, SCN^-), were synthesized based on bipyridine and two novel diimine ligands L1 and L2 (L1 = 1-(4-5′-phenyl-1,3,4-oxadiazolyl-phenyl)-2-pyridinyl-benzoimidazole, L2 = 1-(4-carbazolylphenyl)-2-pyridinylbenzimidazole); and the crystal structure of $[Ru(bpy)_2L1]Cl_2$ was also described. $[Ru(bpy)_2(Pybm)]X_2$ (Pybm = 2-(2-pyridine) benzimidazole) complexes were also prepared as reference samples. In the UV-vis absorption spectra there are one strong $\pi \rightarrow \pi^*$ transition and two $d\pi$ (Ru) $\rightarrow \pi^*$ transitions. By comparisons of photoluminescence properties between $[Ru(bpy)_2L]X$ (**L** = L1, L2) and the reference complexes we find that the complexes with carrier-transporting groups of carbazole and oxadizole have the higher emission intensity and quantum efficiency. One reversible oxidation process in the range 0.80–1.00 V exists in each of the complexes which is assigned to the metal oxidation, $[Ru(III)(bpy)_2L]^{2+} + e^- \rightleftharpoons [Ru(II)(bpy)_2L]^+$.

1. Introduction

In the last few decades a variety of luminescent polypyridyl complexes employing a range of transition metal ions and ligand architectures have been reported. The luminescent and redox properties of Ru (II) complexes of 2,2′-bipyridine (bpy) and related bidentate ligands have been extensively studied due to their significant MLCT absorption in the visible spectral region [1–3], their ability to undergo MLCT excitations [4,5], the relative longevity [6,7] and photoreactivity [8] of the MLCT excited states, the relative inertness of the metal centers in a variety of oxidation states, and the rapidity of redox reactions involving the excited states. These complexes have been employed as building blocks for the design of supramolecular assemblies [9–11], metallodendrimers [12–15], molecular electronics [16,17], molecular machines, molecular motors [18], the fabrication of dye-sensitized solar cells [19,20], and as light harvesting antennas [21,22]. The photophysics, photochemistry, and redox behavior of these complexes are ligand-dependent and therefore can be tuned by judicious choice of the ligands bound to the metal center [23–29]. The basic strategies behind all of these activities are either to introduce different groups within the bipyridine moiety of Ru $(bpy)_3$ or to substitute one or two bipyridine molecule(s) from the $Ru(bpy)_3$ core by other types of donor sites to form mixed ligand tris-chelates to modulate the photo-redox activities of this class of complexes.

Herein, we designed two original diimine ligands, 1-(4-5′-phenyl-1,3,4-oxadiazolyl phenyl)-2-pyridinylbenzoimidazole (L1) and 1-(4-carbazolylphenyl)-2-pyridinylbenzimidazole (L2) by introducing carrier-transporting groups (oxadiazole and carbazole) into 2-(2-pyridine)-benzimidazole (Pybm). Replace one molecule of $Ru(bpy)_3$ core with L1/L2 to produce $[Ru(bpy)_2L]^{2+}$ (**L** = L1, L2) according to the follow three reasons: (i) novel diimine ligands with different ligand-field are applied in molecular design to adjust the molecular orbital energy levels in the Ru (II) complexes which are related to the photochemical, photophysical and electrochemical events and (ii) functional groups with electro-donating or -accepting properties are added into diimine ligands to improve the luminescent properties of Ru (II) complexes and avoiding the triplet–triplet annihilation because of the steric hindrance effect; (iii) the oxadiazole and carbazole moieties can enhance the carrier-transporting properties of the molecular in the devices. The

* Corresponding author. Tel.: +86 25 83596775; fax: +86 25 83314502.
E-mail address: yxzheng@nju.edu.cn (Y. -X. Zheng).

0022-328X/$ – see front matter © 2010 Elsevier B.V. All rights reserved.
doi:10.1016/j.jorganchem.2010.04.037

different anions in these complexes are Cl^-, PF_6^- and SCN^-, [Ru(bpy)$_2$(Pybm)]X_2 (X = Cl^-, PF_6^-, SCN^-) complexes are also synthesized to be used as reference samples.

2. Experimental

2.1. Materials and measurements

Carbazole, ruthenium (III) chloride trihydrate and 2,2′-bipyridine were purchased from Yuan Hang Reagent Company, Kunming Bo Rui metal material Ltd. and Sinopharm Chemical Reagent Co. Ltd. (China), respectively. 1,4-Dibromobenzene, benzoyl hydrazine, 2-(2-pyridyl) benzimidazole (Pybm) and 1,3-dimethyl-3,4,5,6-terahydro-2(1H)-pyrimidinone (DMPU) were brought from Acros, Aldrich and Alfa Companies. All of them were used as received. The IR spectra were taken on a Vector 22 Bruker spectrophotometer (400–4000 cm^{-1}) with KBr pellets. NMR spectra were measured on a Bruker AM 500 spectrometer. Mass spectra were determined with an Autoflex ^{II}TM instrument for MALDI-TOF-MS or on a Varian MAT 311A instrument for ESI–MS. Elemental analyses for C, H, and N were performed on a Perkin–Elmer 240C analyzer. Absorption spectra were measured on a UV-3100 spectrophotometer. Photoluminescence measurements were carried out on Hitachi F4600 luminescence spectrophotometer. The lifetime measurements were measured with an Edinburgh Instruments FLS920P fluorescence spectrometer in solid powder and degassed acetonitrile solution. All the luminescence experiments were prepared in spectroscopic grade solvents. Cyclic voltammetry measurements were conducted on a CHI660b electrochemical analytical instrument, with a polished Pt plate as the working electrode, platinum thread as the counter electrode and Ag/0.1 M $AgNO_3$ in acetonitrile as the reference electrode, tetra-*n*-butylammonium hypherchlorate was used as the supporting electrolyte, using Fc^+/Fc as the internal standard, the scan rate was 0.1 V/s.

The crystal of [Ru(bpy)$_2$L1]Cl_2 suitable for single-crystal X-ray analysis was obtained by diffusion diethyl ether into acetonitrile solution of [Ru(bpy)$_2$L1]Cl_2. The data were collected on a Bruker Smart Apex CCD diffractometer equipped with graphitemonochromated Mo Kα (λ = 0.71073 Å) radiation using a ω-2θ scan mode at 293 K. The highly redundant data sets were reduced using SAINT and absorption corrections were applied using SADABS supplied by Bruker. The structures were solved by direct methods and refined by full-matrix least-squares methods on F^2 using SHELXTL-97.

The luminescence quantum efficiencies were calculated by comparison of the emission intensities (integrated areas) of a standard sample and the unknown sample according to equation (1) [30].

$$\Phi_s = \Phi_{std}\left(\frac{I_s}{I_{std}}\right)\left(\frac{A_{std}}{A_s}\right)\left(\frac{\eta_s}{\eta_{std}}\right)^2 \quad (1)$$

where Φ_s is the luminescence quantum yield of the unknown sample, Φ_{std} is the luminescence quantum yield of the standard substance, the η_s and η_{std} terms represent the refractive indices of the corresponding solvents (pure solvents were assumed), I is the wavelength-integrated area of the corrected emission spectrum, and A is the absorbance value at the excitation wavelength. We take air-free and air-saturated acetonitrile solution of $[Ru(bpy)_3]^{2+}\cdot 2Cl^-$ as standard samples. The Φ_{std} has been revalued to be 9.4% (degassed) or 1.8% (air) [31], ruthenium complexes synthesized were also dissolved in acetonitrile, then were detected under degassed and air-saturated conditions, respectively.

2.2. Synthesis

The chemical structures of the materials used in this work and the synthetic routes were depicted in the Scheme 1. The ligand precursors 2-(4-bromophenyl)-5-phenyl-1,3,4-oxadiazole (**1**) and 1-carbazolyl-4-bromobenzene (**2**) were synthesized as described in literatures [32,33]. Ru(bpy)$_2$$Cl_2\cdot 2H_2O$ was synthesized in advance [34] to be used as the precursor to synthesize all the ruthenium (II) complexes. In preparation of ruthenium (II) complexes, the Schlenk technology was used.

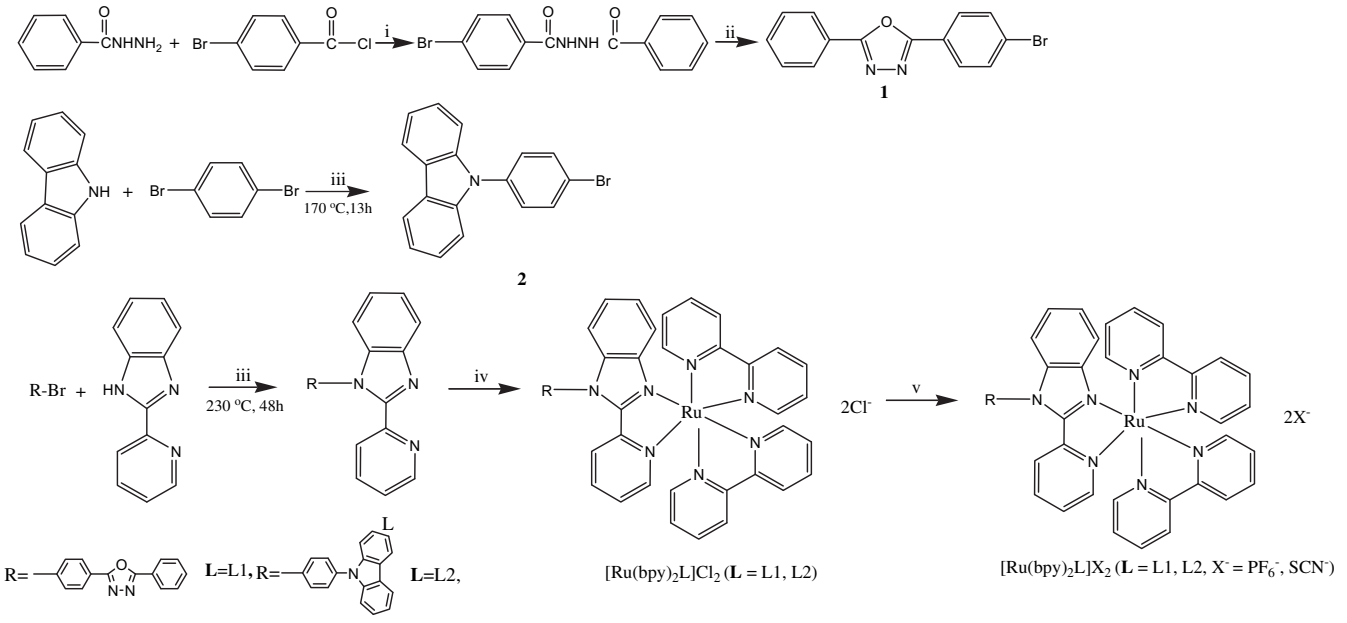

(i) Et_3N, $CHCl_3$, RT; (ii) $POCl_3$, reflux ; (iii) CuI, 18-Crown-6, K_2CO_3, DMPU, in reactor; (iv) Ru(bpy)$_2$$Cl_2\cdot 2H_2O$, ethylene glycol, 120°C, 6h; (v) KPF_6 or KSCN, ethanol, RT or reflux, 2h.

Scheme 1. Synthetic routes for ligands and complexes.

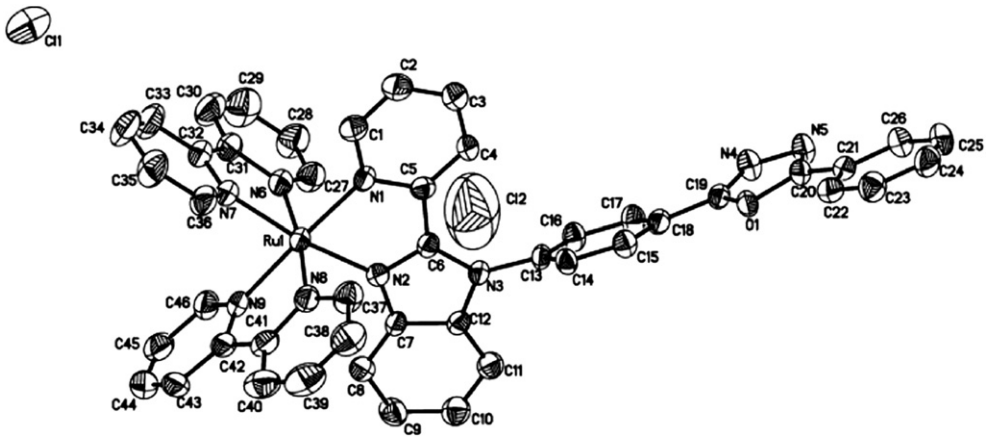

Fig. 1. ORTEP view of complex $[Ru(bpy)_2L1]Cl_2$ with the atom-numbering scheme. Hydrogen atoms are omitted for clarity. Ellipsoids are drawn at the 30% probability level.

2.2.1. Synthesis of 2-(4-bromophenyl)-5-phenyl-1,3,4-oxadiazole (**1**)

4-Bromobenzoyl chloride (21.95 g, 0.1 mol) was added dropwise to a solution of benzoyl hydrazine (13.62 g, 0.1 mol) and triethylamine (10.10 g, 0.1 mol) in chloroform (150 mL) at room temperature (RT). The resulting mixture was stirred for 1 h and then filtered. The collected solid was washed with water and ethanol to give the product N′-benzoyl-4-bromobenzohydrazide (30.32 g, yield: 95%). A mixture of N′-benzoyl-4-bromobenzohydrazide (20.00 g) and $POCl_3$ (250 mL) in a 500 mL flask was refluxed under nitrogen for 5 h. The excessive $POCl_3$ was then distilled out, and the residue was poured into water. The crude solid product was collected by filtration and purified by recrystallization from chloroform/hexane to give 2-(4-bromophenyl)-5-phenyl-1,3,4-oxadiazole (**1**) as white needlelike crystals (16.04 g, yield: 85%). M. p.: 164–168 °C. IR (KBr, cm^{-1}): 3060, 1600, 1546, 1474, 1073, 728, 689. ^1H NMR ($CDCl_3$, 500 MHz): δ 8.159 (d, 2H, J = 7 Hz), 8.040 (d, 2H, J = 9 Hz), 7.710 (d, 2H, J = 8.5 Hz), 7.570 (m, 3H). MS(ESI): m/z 301.08 $[M]^+$. Anal. Calcd for $C_{14}H_9N_2OBr$: C, 55.84; H, 3.01; N, 9.30. Found: C, 55.87; H, 3.11; N, 9.27.

Table 1
Crystallographic Data for $[Ru(bpy)_2L1]Cl_2$.

	$[Ru(bpy)_2L1]Cl_2$
Formula	$C_{46}H_{33}N_9OCl_2Ru$
FW	899.78
T (K)	271(2)
Wavelength (Å)	0.71073
Crystal system	Monoclinic
Space group	$P\,2_1/c$
a (Å)	11.320(4)
b (Å)	35.314(12)
c (Å)	13.017(4)
α (deg)	90.00
β (deg)	105.481(6)
γ (deg)	90.00
V (Å^3)	5015(3)
Z	4
ρ_{calcd} (g/cm^3)	1.192
μ (Mo Kα) (mm^{-1})	0.459
F (000)	1832
Range of transm factors (deg)	2.31–19.35
Reflns collected	27 313
Unique	9781
Data/restraints/params	9781/0/532
GOF on F^2	0.873
R_1^a, $wR_2^b[I > 2\sigma(I)]$	0.0559, 0.1311
R_1^a, wR_2^b(all data)	0.1157, 0.1475
CCDC No.	759 108

$R_1^a = |\sum||F_o| - |F_c|/\sum F_o||$. $wR_2^b = [\sum w(F_o^2 - F_c^2)^2/\sum w(F_o^2)]^{1/2}$

2.2.2. Synthesis of 1-carbazolyl-4-bromobenzene (**2**)

Similar methods (see Scheme 1) are used to prepare **2**, L1 and L2. A mixture of carbazole (16.72 g, 0.1 mol), 1,4-dibromobenzene (23.59 g, 0.1 mol), CuI (1.90 g, 0.01 mol), 18-Crown-6 (0.88 g, 0.0033 mol), K_2CO_3 (27.67 g, 0.2 mol) and DMPU (3 mL) was put into a reactor, then keep it heating at 170 °C for 13 h under nitrogen. After cooling to room temperature, the mixture was quenched with 1 N HCl, the precipitate was filtered and washed with $NH_3\cdot H_2O$ and water. The brown solid was purified with column chromatography using hexane as eluant (10.95 g, yield: 34%). M. p.: 152–154 °C. IR (KBr, cm^{-1}): 3056, 1496, 1452, 1230, 751. ^1H NMR ($CDCl_3$, 500 MHz): δ 8.175 (d, 2H, J = 7 Hz), 7.757 (d, 2H, J = 8.5 Hz), 7.495 (d, 2H, J = 8.5 Hz), 7.431 (t, 2H, J = 7 Hz), 7.411 (d, 2H, J = 9 Hz), 7.342 (t, 2H, J = 7.5 Hz). MS(MALDI-TOF): m/z 321.035 $[M]^+$. Anal. Calcd. for $C_{18}H_{12}NBr$: C, 67.10; H, 3.75; N, 4.35. Found: C, 66.93; H, 3.71; N, 4.31.

2.2.3. Synthesis of 1-(4-5′-phenyl-1,3,4-oxadiazolylphenyl)-2-pyridinylbenzoimidazole (L1)

The procedure is similar to that of compound **2** with the materials of **1** (3.01 g, 0.01 mol) and Pybm (1.95 g, 0.01 mol) at the temperature of 230 °C (2.50 g, yield: 60%). M. p.: 186–189 °C. IR (KBr, cm^{-1}): 3050, 1606, 1500, 1442, 1385, 773, 755, 741, 708, 691. ^1H NMR ($CDCl_3$, 500 MHz): δ 8.380 (d, 3H, J = 7.5 Hz), 8.200 (d, 2H, J = 7.5 Hz), 7.987 (t, 1H, J = 7.5 Hz), 7.603–7.577 (m, 7H), 7.525 (t, 2H, J = 7.5 Hz), 7.405 (t, 1H, J = 6 Hz), 7.321(d, 1H, J = 8.5 Hz). MS (MALDI-TOF): m/z 416.232 $[M]^+$. Anal. Calcd. for $C_{26}H_{17}N_5O$: C, 75.17; H, 4.12; N, 16.86. Found: C, 75.11; H, 4.21; N, 16.81.

2.2.4. Synthesis of 1-(4-carbazolylphenyl)-2-pyridinylbenzimidazole (L2)

The procedure is similar to that of compound **2** with the materials of **2** (3.22 g, 0.01 mol) and Pybm (1.95 g, 0.01 mol) at the temperature of 230 °C (2.93 g, yield: 67%). M. p.: 225–228 °C. IR (KBr, cm^{-1}): 3044, 1728, 1593, 1514, 1446, 740. ^1H NMR ($CDCl_3$, 500 MHz): δ 8.489 (d, 2H, J = 4.5 Hz), 8.203 (d, 2H, J = 7.5 Hz), 8.074 (d, 1H, J = 8 Hz), 7.906 (t, 1H, J = 7.5 Hz), 7.762 (d, 2H, J = 8.5 Hz), 7.614 (d, 2H, J = 9 Hz), 7.550 (d, 2H, J = 7.5 Hz), 7.502 (t, 3H, J = 7 Hz), 7.472 (m, 2H), 7.357 (t, 3H, J = 7 Hz). MS (MALDI-TOF): m/z 437.130 $[M]^+$. Anal. Calcd for $C_{30}H_{20}N_4$: C, 82.55; H, 4.62; N, 12.84. Found: C, 82.54; H, 4.69; N, 12.83.

2.2.5. Synthesis of $Ru(bpy)_2Cl_2\cdot 2H_2O$

The following modified method [34] was utilized to prepare this complex with good yields. Commercial $RuC1_3\cdot 3H_2O$ (3.92 g, 15.0 mmol), bipyridine (4.69 g, 30.0 mmol), and LiCl (3.04 g, 100.0 mmol) were refluxed and stirred in reagent grade

Table 2
Selected bond lengths (Å) and angles (°) for $[Ru(bpy)_2L1]Cl_2$.

Ru(1)–N(6)	2.054(4)	Ru(1)–N(8)	2.054(4)
Ru(1)–N(9)	2.061(4)	Ru(1)–N(7)	2.069(4)
Ru(1)–N(2)	2.069(4)	Ru(1)–N(1)	2.074(4)
N(6)–Ru(1)–N(8)	172.3(2)	N(6)–Ru(1)–N(9)	95.0(2)
N(8)–Ru(1)–N(9)	78.9(2)	N(6)–Ru(1)–N(7)	79.4(2)
N(8)–Ru(1)–N(7)	95.2(2)	N(9)–Ru(1)–N(7)	85.0(2)
N(6)–Ru(1)–N(2)	95.8(2)	N(8)–Ru(1)–N(2)	90.1(2)
N(9)–Ru(1)–N(2)	101.5(2)	N(7)–Ru(1)–N(2)	172.4(2)
N(6)–Ru(1)–N(1)	89.2(2)	N(8)–Ru(1)–N(1)	96.9(2)
N(9)–Ru(1)–N(1)	175.8(2)	N(7)–Ru(1)–N(1)	96.1(2)
N(2)–Ru(1)–N(1)	77.7(1)		

dimethylformamide (50 mL) for 8 h. After the reaction mixture was cooled to room temperature, 250 mL of reagent grade acetone was added and the resultant solution was kept at 0 °C overnight. Filtering yielded a dark green-black microcrystalline product. The solid was washed three times with 25-mL portions of water, three 25-mL portions of diethyl ether, and then dried by suction to give 4.82 g of $Ru(bpy)_2Cl_2.2H_2O$ (yield: 61.8%).

*2.2.6. General preparation of $[Ru(bpy)_2L]Cl_2$ (**L** = L1, L2)*

$Ru(bpy)_2Cl_2\cdot 2H_2O$ (0.06 g, 0.12 mmol) and **L** (0.15 mmol) were heated under N_2 atomsphere at 120 °C for 6 h in ethylene glycol until the color of the solution thoroughly changed to be red. After the mixture was cooled to RT, the solvent was distilled out. The resulting red solid was purified by alumina column chromatography with methanol/dichloromethane (v/v = 0–5%) as eluant to get $[Ru(bpy)_2L]Cl_2$ complexes.

*2.2.7. General preparation of $[Ru(bpy)_2L](PF_6)_2$ (**L** = L1, L2)*

The crude product $[Ru(bpy)_2L]Cl_2$ (0.12 mmol) used as precursor complex was resolved in 10 mL ethanol. KPF_6 (0.22 g, 1.2 mmol) aqueous solution was added dropwise into the ethanol solution of $[Ru(bpy)_2L]Cl_2$. The solution was stirred for 2 h at room temperature, and then filtered to get the precipitation. This crude product was purified by alumina column chromatography with methanol/dichloromethane (v/v = 0–5%) as eluant to get $[Ru(bpy)_2L](PF_6)_2$ complexes.

*2.2.8. General preparation of $[Ru(bpy)_2L](SCN)_2$ (**L** = L1, L2)*

The synthesis of $[Ru(bpy)_2L](SCN)_2$ is similar to the process of $[Ru(bpy)_2L](PF_6)_2$, the aqueous solution of KPF_6 was replaced by KSCN (0.23 g, 2.4 mmol), and the mixed solution was refluxed 2 h. The solution was concentrated to get the crude product which was purified by alumina column chromatography with methanol/dichloromethane (v/v = 0–5%) as eluant to get $[Ru(bpy)_2L](SCN)_2$ complexes.

2.2.9. General preparation of $[Ru(bpy)_2(Pybm)]X_2$ ($X = Cl^-$, PF_6^-, SCN^-)

The processes resemble the preparations of $[Ru(bpy)_2L]X_2$. It is needed to point out that because of the light sensitivity of $[Ru(bpy)_2(Pybm)]X_2$, the purified products were gained through recrystallization twice from diethyl ether and acetonitrile instead of using chromatograph.

$[Ru(bpy)_2L1]Cl_2$ (0.05 g, yield: 46.0%) ^{1}H NMR (500 MHz, D_2O) δ 8.66–8.59 (m, 3H), 8.59–8.50 (m, 3H), 8.27–8.20 (m, 2H), 8.18 (d, J = 8.0 Hz, 1H), 8.12 (t, J = 8.6 Hz, 2H), 8.09–8.03 (m, 2H), 8.00 (t, J = 6.0 Hz, 2H), 7.87 (dd, J = 13.1, 4.1 Hz, 2H), 7.83 (d, J = 5.4 Hz, 1H), 7.81–7.78 (m, 1H), 7.76 (d, J = 8.2 Hz, 1H), 7.70–7.62 (m, 3H), 7.55–7.41 (m, 5H), 7.37 (t, J = 6.7 Hz, 3H), 7.32 (d, J = 8.4 Hz, 1H), 7.16 (t, J = 7.8 Hz, 1H). MS(ESI): m/z 864.17 $[M - Cl]^+$.

$[Ru(bpy)_2L1](PF_6)_2$ (0.04 g, yield: 31.1%) ^{1}H NMR (500 MHz, CD_3CN) δ 8.56–8.47 (m, 6H), 8.21 (d, J = 7.5 Hz, 2H), 8.15 (t, J = 7.5 Hz, 1H), 8.08 (t, J = 9.0 Hz, 3H), 8.03 (d, J = 9.0 Hz, 2H), 7.97 (dd, J = 2, 2.5 Hz, 2H), 7.84 (m, 2H), 7.77–7.74 (m, 2H), 7.72–7.71 (m, 1H), 7.67–7.62 (m, 3H), 7.48–7.39 (m, 5H), 7.34–7.28 (m, 3H), 7.14 (t, J = 8.25 Hz, 1H). MS(ESI): m/z 974.17 $[M - PF_6]^+$.

$[Ru(bpy)_2L1](SCN)_2$ (0.05 g, yield: 44.9%) ^{1}H NMR (500 MHz, CD_3CN) δ 8.62–8.46 (m, 6H), 8.20 (dd, J = 12.1, 5.5 Hz, 2H), 8.17–8.11 (m, 1H), 8.10–8.05 (m, 2H), 8.03 (dd, J = 6.6, 2.7 Hz, 2H), 7.97 (dd, J = 11.7, 3.5 Hz, 2H), 7.88–7.81 (m, 2H), 7.80–7.70 (m, 3H), 7.68–7.59 (m, 3H), 7.51–7.46 (m, 3H) 7.44–7.41 (m, 3H), 7.36–7.25 (m, 3H), 7.12 (t, J = 7.8 Hz, 1H). MS(ESI): m/z 887.17 $[M - SCN]^+$.

$[Ru(bpy)_2L2]Cl_2$ (0.04 g, yield: 38.8%) ^{1}H NMR (500 MHz, D_2O) δ 8.66–8.60 (m, 3H), 8.56 (d, J = 8.1 Hz, 1H), 8.26 (d, J = 7.7 Hz, 2H), 8.20 (td, J = 8.1, 1.2 Hz, 1H), 8.12 (t, J = 7.9 Hz, 2H), 8.09–7.99 (m, 6H), 7.92–7.83 (m, 4H), 7.81 (d, J = 5.2 Hz, 1H), 7.72 (d, J = 8.3 Hz, 2H), 7.58–7.52 (m, 4H), 7.52–7.43 (m, 5H), 7.42–7.35 (m, 4H), 7.21–7.14 (m, 1H). MS(ESI): m/z 909.00 $[M - Cl + Na]^{2+}$.

$[Ru(bpy)_2L2](PF_6)_2$ (0.09 g, yield: 65.4%) ^{1}H NMR (500 MHz, CD_3CN) δ 8.57–8.53 (m, 3H), 8.49 (d, J = 7.5 Hz, 1H), 8.24 (d, J = 8 Hz, 2H), 8.16 (t, J = 7.75 Hz, 3H), 8.08–8.02 (m, 5H), 8.01–7.95 (m, 3H), 7.86–7.83 (m, 3H), 7.79 (d, J = 4.5 Hz, 1H), 7.76 (d, J = 5.5 Hz, 1H), 7.53–7.50 (m, 4H), 7.48–7.43 (m, 3H), 7.41–7.39

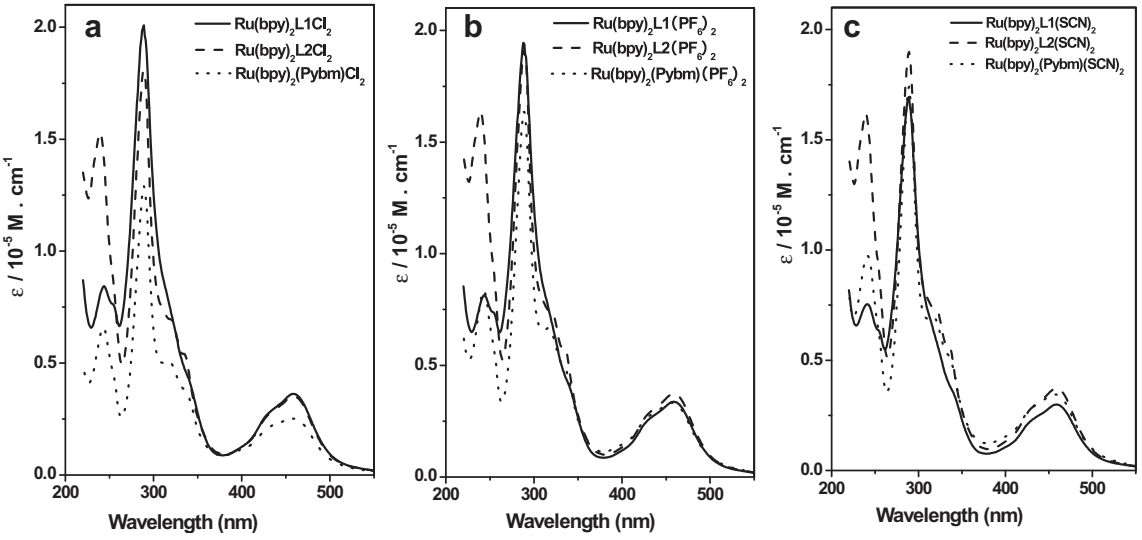

Fig. 2. Electronic absorption spectra of all the ruthenium (II) complexes in acetonitrile solution at room temperature.

Table 3
Absorption and photoluminescence data of ruthenium (II) complexes in solution and solid state at room temperature.

Complex	Medium	$\lambda_{abs,max}$ (nm) $\varepsilon(\times 10^5$ M cm$^{-1})$	Emission λ_{max} (nm)[a]	Lifetime τ	Efficiency Φ (%)
$[Ru(bpy)_2L1]Cl_2$	Solid		670[b]	2.003 μs[d] $\chi^2 = 0.976$	[f]
	CH_3CN	288, 2.01	648[c]	264.18 ns[e] $\chi^2 = 0.997$	5.2[g] 1.4[h]
$[Ru(bpy)_2L1](PF_6)_2$	Solid		650[b]	2.280 μs[d] $\chi^2 = 0.980$	[f]
	CH_3CN	286, 1.95	650[c]	269.90 ns[e] $\chi^2 = 0.997$	3.4[g] 0.84[h]
$[Ru(bpy)_2L1](SCN)_2$	Solid		660[b]	2.214 μs[d] $\chi^2 = 0.982$	[f]
	CH_3CN	288, 1.69	647[c]	257.20 ns[e] $\chi^2 = 0.997$	5.6[g] 1.8[h]
$[Ru(bpy)_2L2]Cl_2$	Solid		653[b]	2.236 μs[d] $\chi^2 = 0.980$	[f]
	CH_3CN	287, 1.80	643[c]	263.70 ns[e] $\chi^2 = 0.997$	4.8[g] 1.2[h]
$[Ru(bpy)_2L2](PF_6)_2$	Solid		654[b]	2.340 μs[d] $\chi^2 = 0.980$	[f]
	CH_3CN	289, 1.91	643[c]	247.68 ns[e] $\chi^2 = 0.998$	3.7[g] 0.92[h]
$[Ru(bpy)_2L2](SCN)_2$	Solid		663[b]	2.222 μs[d] $\chi^2 = 0.979$	[f]
	CH_3CN	288, 1.90	643[c]	238.79 ns[e] $\chi^2 = 0.998$	9.7[g] 2.6[h]
$[Ru(bpy)_2(Pybm)]Cl_2$	Solid		643[b]	2.402 μs[d] $\chi^2 = 0.981$	[f]
	CH_3CN	289, 1.29	638[c]	151.44 ns[e] $\chi^2 = 0.997$	1.8[g] 0.71[h]
$[Ru(bpy)_2(Pybm)](PF_6)_2$	Solid		651[b]	2.257 μs[d] $\chi^2 = 0.982$	[f]
	CH_3CN	287, 1.63	628[c]	125.07 ns[e] $\chi^2 = 0.998$	3.2[g] 0.75[h]
$[Ru(bpy)_2(Pybm)](SCN)_2$	Solid		625[b]	2.044 μs[d] $\chi^2 = 0.978$	[f]
	CH_3CN	289, 1.74	634[c]	114.31 ns[e] $\chi^2 = 0.997$	3.3[g] 0.66[h]

[a] Emission maxima from not corrected spectra.
[b] Be excited at 495 nm.
[c] Be excited at 376 nm.
[d] Be detected at $\lambda_{ex} = 495$ nm and the maximal emission bands of the ruthenium (II) complexes in solid state.
[e] Be detected at $\lambda_{ex} = 405$ nm and the maximal emission bands of the ruthenium (II) complexes in degassed acetonitrile solution.
[f] Not detected.
[g] Calculated by $\Phi_s = \Phi_{std}(I_s A_{std}\eta_s^2)/(I_{std}A_s\eta_{std}^2)$ using degassed acetonitrile solution of $[Ru(bpy)_3]^{2+}\cdot 2Cl^-$ as a standard sample ($\Phi_{std} = 9.4\%$), the error in this method is estimated to be approximately 10% of the measured value.
[h] Calculated by $\Phi_s = \Phi_{std}(I_s A_{std}\eta_s^2)/(I_{std}A_s\eta_{std}^2)$ using air-saturated acetonitrile solution of $[Ru(bpy)_3]^{2+}\cdot 2Cl^-$ as a standard sample ($\Phi_{std} = 1.8\%$), the error in this method is estimated to be approximately 10% of the measured value.

(m, 3H), 7.38–7.33 (m, 3H), 7.15 (t, $J = 7.25$ Hz, 1H). MS(ESI): m/z 995.33 $[M - PF_6]^+$.

$[Ru(bpy)_2L2](SCN)_2$ (0.05 g, yield: 40.4%) ^1H NMR (500 MHz, CD_3CN) δ 8.65 (d, $J = 8.2$ Hz, 3H), 8.58 (d, $J = 8.1$ Hz, 1H), 8.25 (d, $J = 7.8$ Hz, 2H), 8.23–8.18 (m, 1H), 8.13 (t, $J = 8.0$ Hz, 2H), 8.11–8.07 (m, 2H), 8.06–8.00 (m, 4H), 7.93–7.84 (m, 4H), 7.82 (d, $J = 5.5$ Hz, 1H), 7.72 (d, $J = 8.2$ Hz, 2H), 7.54 (dd, $J = 8.1$, 7.3 Hz, 4H), 7.51–7.45 (m, 5H), 7.44–7.34 (m, 4H), 7.18 (t, $J = 7.7$ Hz, 1H). MS (ESI): m/z 908.92 $[M - SCN]^+$.

3. Results and discussion

3.1. Crystallograph

The X-ray crystal structure of $[Ru(bpy)_2L1]Cl_2$ is shown in Fig. 1, and the crystal data are presented in Table 1, selected bond lengths and angles are given in Table 2. Crystal of $[Ru(bpy)_2L1]Cl_2$ was found to be monoclinic and the crystallographic data were refined in space group $P2_1/c$. The geometry of the ruthenium (II) center is distorted octahedral. A slight distortion from octahedral geometry is reflected in *trans*-N-Ru-N bond angles below 180° (175.8(2), 172.4 (2) and 172.3(2), respectively) and *cis*-N-Ru-N angles below 90° (77.7(1), 79.4(2) and 78.9(2), respectively) which agree with the reported literature [35]. The N–Ru–N "bite" angles for the bidentate ligands are typical of 5-membered chelate rings formed by such ligands. The two Ru–N bond distances for the same diimine ligand are similar (2.074(4) Å for Ru–N(1) and 2.069(4) Å for Ru–N (2), for example). The Ru–N bond lengths found in $[Ru(bpy)_2L1]Cl_2$ (2.054(4)-2.074(4) Å) are in agreement with those for related structures [36–39]. There are lattice water molecules in this complex which are significantly disordered and could not be modeled properly with the program SQUEEZE [40], a part of the PLATON package [41]. The number of lattice water molecules can be calculated to be four depending on the TGA curve of this complex (Fig. S3).

3.2. Photoluminescence properties

The electronic absorption spectra of all the nine ruthenium (II) complexes studied in acetonitrile solution are shown in Fig. 2 and all the peaks data are listed in Table 3. The presence of different acceptor levels in the complexes may be responsible for the observed multiple absorptions [42]. All compounds show a strong ligand centered $\pi \rightarrow \pi^*$ transition and two metal-to-ligand charge-transfer ($d\pi$ (Ru) $\rightarrow \pi^*$, MLCT) transitions in the UV-visible range. The band at ~285 nm has been assigned to LC $\pi \rightarrow \pi^*$ transitions by comparison with the spectrum of protonated bipyridine [43] and corresponding free ligands (L1, L2 and Pybm, see Supporting Information). The two remaining intense bands at ~240 and 460 nm have been assigned to MLCT $d\pi$ (Ru) $\rightarrow \pi^*$ transitions. With respect to the C_2 axis of the bipyridine ligand, there are two different kinds of bipyridine acceptor orbitals, one symmetric (χ) and one antisymmetric (ψ) and the transitions from metal-filled $d\pi$ orbitals to these two π^* orbitals result in the above-mentioned bands. Thus these are believed to represent MLCT transitions and are expected for low-spin ruthenium (II) complexes. The lower-energy band at ~460 nm is considered to be the $d\pi(Ru) \rightarrow \pi^*(\psi)$ transition and the higher-energy band near 240 nm due to the $d\pi$ (Ru) $\rightarrow \pi^*(\chi)$ transition [43]. The MLCT absorption maxima of all the compounds with replaced new diimine ligand(s) show little red shift from 451 nm of the pristine $[Ru(bpy)_3]^{2+}$ to longer wavelengths. From the Fig. 2, it is also observed that the absorption intensities of all the $[Ru(bpy)_2L]X_2$ (**L** = L1, L2, X = Cl^-, PF_6^-, SCN^-) are stronger than the reference complexes $[Ru(bpy)_2(Pybm)]X_2$ (X = Cl^-, PF_6^-, SCN^-). It is reasonable to infer that the addition of carrier-transporting groups (oxadiazole and carbazole) is useful to enhance the electronic absorption of ruthenium (II) ploypyridine complexes. This benefit is certified in quantum efficiency in following discussion.

Fig. 3 demonstrates the emission spectra of the nine ruthenium (II) complexes in air-equilibrated acetonitrile solution and in solid state excited at 376 nm and 495 nm at room temperature, respectively. Emission band maxima (λ_{max}), emission quantum yield (Φ), and lifetime (τ) values are also collected in Table 3. It is easily to find that the ruthenium (II) complexes in acetonitrile solution excited at 376 nm lead to the emissions around 630–650 nm and these complexes in solid state excited at 495 nm lead to the emissions around 640–670 nm which are the typical MLCT emission of ruthenium (II) polypyridine complexes. Unlike the absorption spectra, the emission spectra of these compounds show bigger variation in both intensity and peak position. From Fig. 3 we can

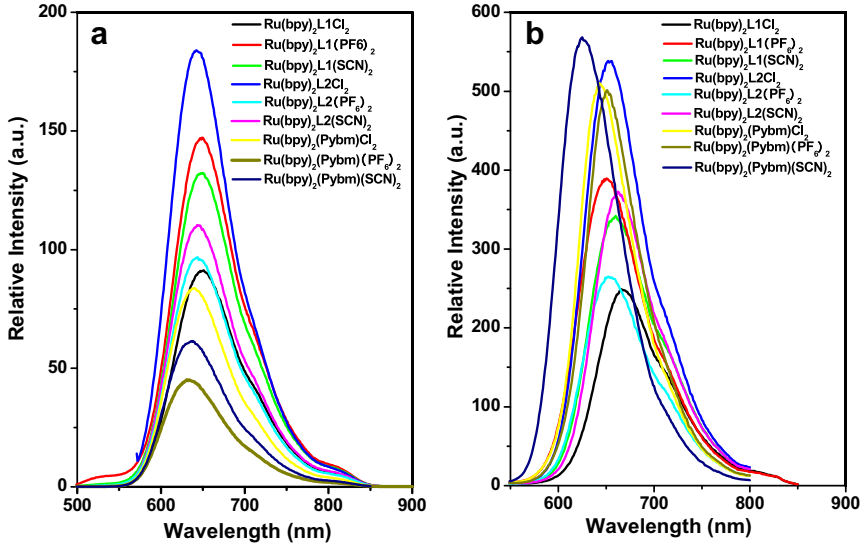

Fig. 3. Emission spectra of all the ruthenium (II) complexes in acetonitrile solution (a, λ_{ex} = 376 nm) and solid (b, λ_{ex} = 495 nm) state at room temperature.

observe that the complexes with two novel diimine ligands [Ru(bpy)$_2$L]X$_2$ (**L** = L1, L2, X = Cl$^-$, PF$_6^-$, SCN$^-$) show higher intensities than the reference complexes [Ru(bpy)$_2$(Pybm)]X$_2$ (X = Cl$^-$, PF$_6^-$, SCN$^-$). After introducing the carrier-transporting groups into the Pybm the derivatives become much more rigid and also can provide efficient shielding of the Ru (II) core towards external quenching which are favorable for the light emission. Compared to the emission band at 606 nm of [Ru(bpy)$_3$]$^{2+}$ in acetonitrile solution [43], the emission bands of all the ruthenium (II) complexes in this article have a little red shift. A similar red shift in the absorption and the emission has been detected in several mixed-ligand Ru complexes in which the emitting ligand has lower π^* energies than

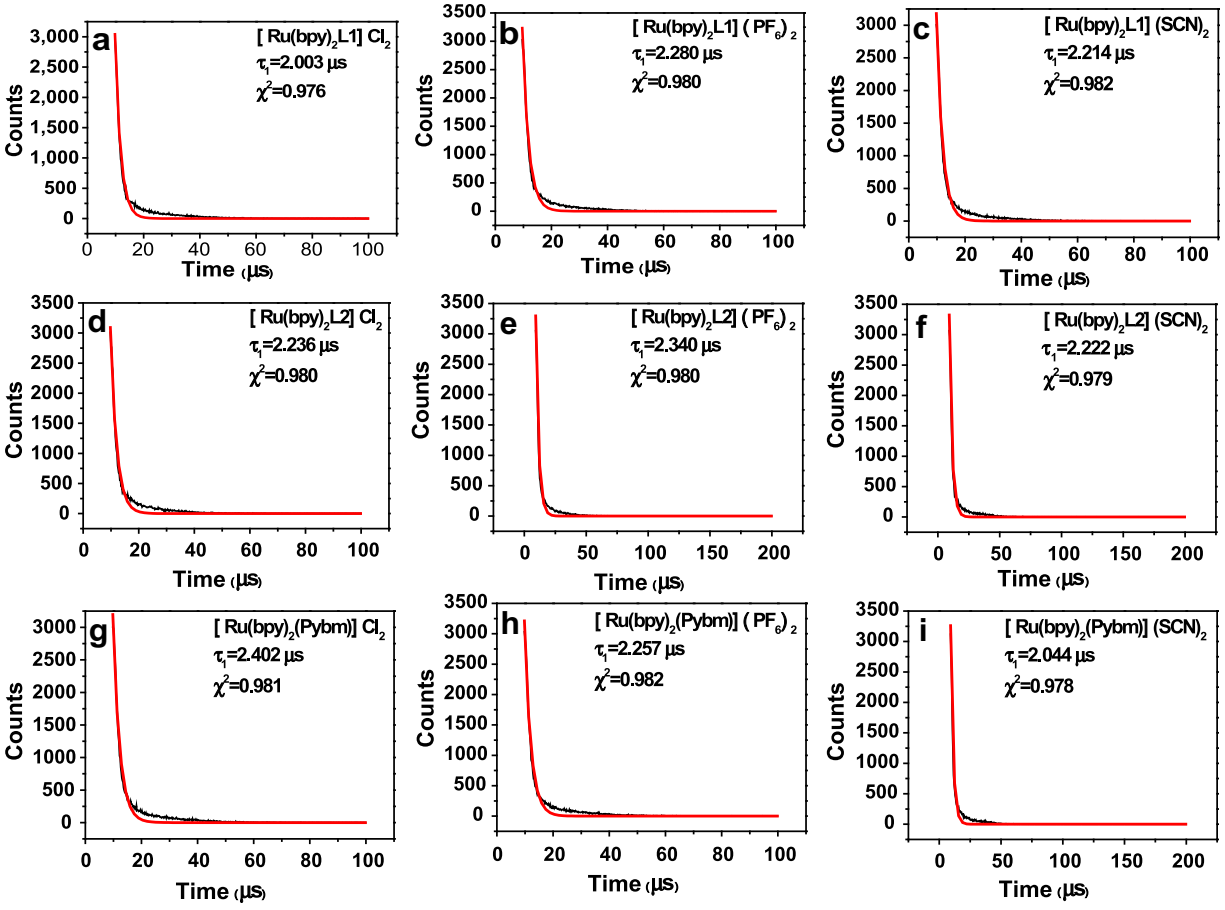

Fig. 4. Decay curves of all the ruthenium (II) complexes in solid state at room temperature.

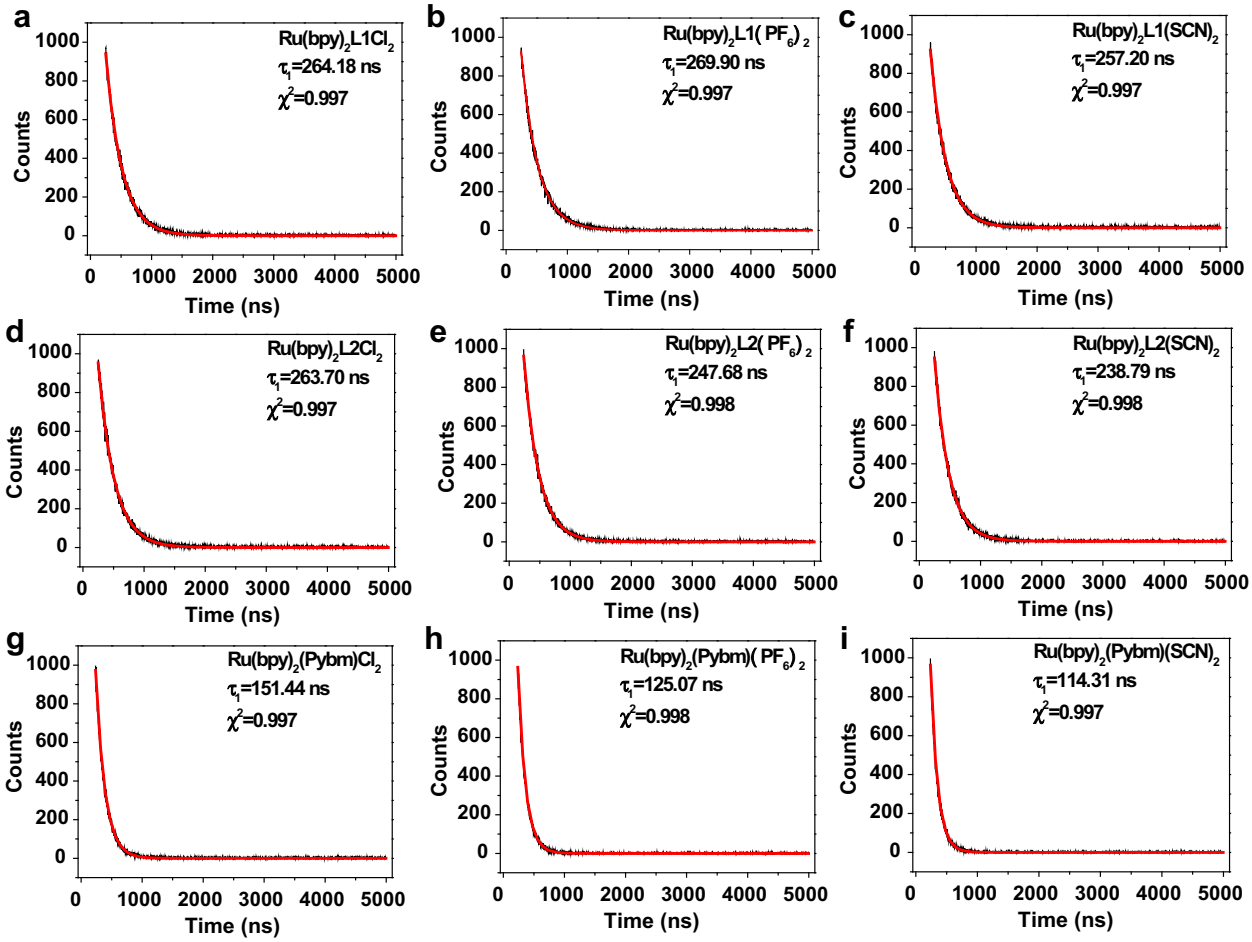

Fig. 5. Decay curves of all the ruthenium (II) complexes in degassed acetonitrile solution at room temperature. The black lines are experimental lines and the red lines are fitting lines.

the ligand it replaced [44,45]. The replaced ligands in our case are the ones with electron-accepting groups (oxadiazole) or electron-donating groups (carbazole). By compared with the reference complexes $[Ru(bpy)_2(Pybm)]X_2$ ($X = Cl^-$, PF_6^-, SCN^-), the red shift also exists, so both of the oxadiazole and carbazole can increase the ground state (t_{2g}) energy level of the complex. These two novel diimine ligands lose the excellent symmetry of bipyridine. The resulting degeneration of the excited states also seems to lead to red-shifted emission [46].

The luminescence quantum yield, defined as the ratio of the number of photons emitted to the number of photons absorbed, gives the efficiency of the luminescence process. From Table 3 it is noticed that the quantum efficiencies of $[Ru(bpy)_2L]X_2$ (**L** = L1, L2) are higher than that of the reference complexes $[Ru(bpy)_2(Pybm)]X_2$ either in degassed solutions or in air-saturated ones, and similar to the emission intensity sequence as the above description. However, the change of anions, $X = Cl^-$, PF_6^-, SCN^-, has no distinct effect in emission intensity and quantum efficiency yield suggesting that the anions did not affect emission process greatly. We think that because the anions are located at outside of the Ru-core and the strengths of Ru–X bonds are weaker than that of Ru–N. We also observe a significant decrease in the quantum efficiencies of these complexes relative to the standard sample, $[Ru(bpy)_3]^{2+}\cdot 2Cl^-$, except the sample $[Ru(bpy)_2L2](SCN)_2$. Because there were also

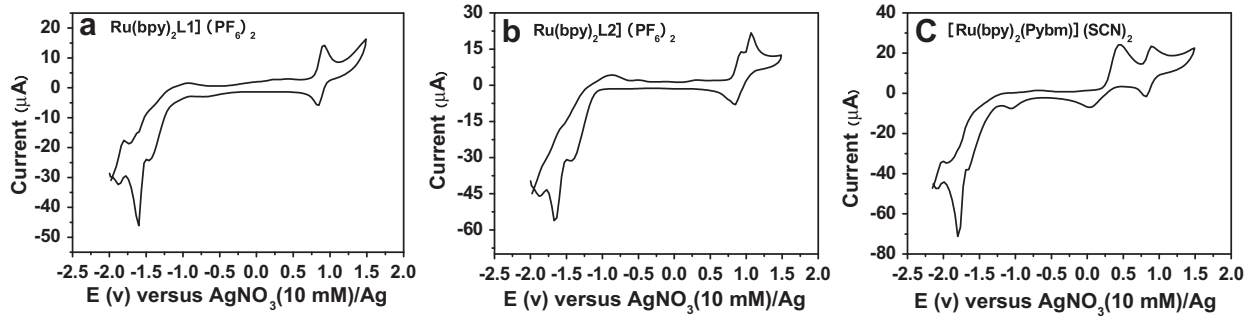

Fig. 6. Cyclic voltammograms of ruthenium (II) complexes in acetonitrile solution at 298 K.

Table 4
Electrochemical data of ruthenium (II) complexes at 298 K.

Complex	Ru(III)-Ru(II)	Ligand reduction	$\Delta E^o(v)$[a]	ν_{MLCT} (cm^{-1})	
	E^o_{298} (v) (ΔEp (mv))	E^o_{298} (v)		Cal.[b]	Obs.[c]
$[Ru(bpy)_2L1]Cl_2$	0.83 (80)	−1.60	2.43	22 598	21 834
$[Ru(bpy)_2L1](PF_6)_2$	0.84 (60)	−1.60	2.44	22 679	21 786
$[Ru(bpy)_2L1](SCN)_2$	0.85 (70)	−1.63	2.48	23 001	21 834
$[Ru(bpy)_2L2]Cl_2$	0.85 (60)	−1.64	2.49	23 082	21 786
$[Ru(bpy)_2L2](PF_6)_2$	0.84 (90)	−1.66	2.50	23 163	21 786
$[Ru(bpy)_2L2](SCN)_2$	0.82 (100)	−1.60	2.42	22 517	21 834
$[Ru(bpy)_2(Pybm)]Cl_2$	0.81 (90)	−1.80	2.61	24 050	21 881
$[Ru(bpy)_2(Pybm)](PF_6)_2$	0.81 (90)	−1.80	2.61	24 050	21 834
$[Ru(bpy)_2(Pybm)](SCN)_2$	0.82 (80)	−1.78	2.60	23 969	21 929

[a] Calculated by using eqn (3) of the text.
[b] Calculated by using eqn (2) of the text.
[c] In acetonitrile solution.

significant red shifts in the emission of these complexes, these decreased quantum yields are probably a direct consequence of the energy gap law [47].

The decay of an excited state takes place by competitive radiative and non-radiative processes, which is an important parameter for practical applications of luminescence. In this study, the luminescence decay curves of all the complexes in solid state were obtained from time-resolved luminescence experiments at the MLCT excitation and maximal emission wavelengths at room temperature (Fig. 4), the luminescence decay curves of all the samples in degassed acetonitrile solution were also obtained from time-resolved luminescence experiments using the laser lamp as the light source (λ_{ex} = 405 nm) and emitting at the maximal wavelength (Fig. 5). From the figures we can find that the emission decay curves of the nine complexes are best fitted by mono-exponential, which lie on the microsecond timescale. If a decay is not single exponential then that implies that there are different sites for the ion and that each site has a different lifetime. So, from our results we can conclude that all ruthenium ions occupy the same average local environment within each sample. Fig. 5 also shows the mono-exponential decay curves, but the lifetimes in degassed acetonitrile solution are much shorter than in solid state, the quenching of solvent may account for this. The lifetimes of the reference samples are shorter than $[Ru(bpy)_2L]X_2$, that support the sequence of quantum efficiency.

3.3. Redox properties

Using a platinum working electrode, redox properties of the complexes have been studied in acetonitrile solution by cyclic voltammetry (CV). Complexes are electroactive with respect to metal as well as ligand centers. Representative voltammograms are shown in Fig. 6 and the electrochemical data are depicted in Table 4.

One reversible oxidation process in the range 0.80–1.00 V exists in each of the complexes which is assigned to the metal oxidation, $[Ru(III)(bpy)_2L]^{2+} + e^- \rightleftharpoons [Ru(II)(bpy)_2L]^+$. Under the experimental condition using saturated calomel electrode (SCE) as inner reference electrode, the Ru (III)–Ru (II) reduction potential of $[Ru(bpy)_3]^{2+}$ appears at 1.29 V [48,49], so this assignment is reasonable.

In some voltammograms of these complexes (Fig. 6 and Fig. S2), some other oxidation processes could be found in the range 0–1.5 V. These irreversible oxidation processes may be due to either Ru (III)–Ru (IV) oxidation or oxidation of the coordinated ligand [50]. 2,2′-bipyridine is a well known potential electron-transfer center and each bipyridine can accept two electrons in one electrochemically accessible LUMO [51]. Since all the complexes have two bipyridine units, four one-electron reductions are therefore expected. However, in practice we have observed only one reduction process in the range −1.60 ∼ −1.80 V. Other expected reductions could not be seen possibly due to solvent cut-off. Other irreversible reduction waves in some figures may be due to the presence of water and impurities in acetonitrile.

The lowest energy MLCT transition involves excitation of the electron from the filled t_{2g}^6 orbital of ruthenium (II) to the lowest π^* orbital of the bipyridine ligand. Now the associated energy of the MLCT band for each complex can be predicted from the experimentally observed electrochemical data by considering the following two eqns (2) and (3) [52,53].

$$\nu_{MLCT} = 8065(\Delta E) + 3000 \quad (2)$$

$$\Delta E = E_{298}(Ru(III)/Ru(II)) - E_{298}(L) \quad (3)$$

Here, E_{298} (Ru(III)/Ru(II)) and E_{298} (**L**) are the formal potentials (in V) of the ruthenium (III)–ruthenium (II) couple and the first ligand reduction, respectively. The ν_{MLCT} is the frequency of the lowest energy MLCT transition (in cm^{-1}). The factor 8065 in eqn (2) is used to convert potential difference ΔE from volt to cm^{-1} and the term 3000 cm^{-1} is of empirical origin. The calculated values accord with the experimental observed MLCT energies (Table 4) in a certain degree. This agreement is previously reported in the other mixed ligand ruthenium bipyridine complexes and other related systems [54–56].

4. Conclusion

The noteworthy feature of our work is success in introducing two diimine ligands with carrier-transporting units of oxadiazole and carbazole into ruthenium (II) bipyridine complexes. The comparisons of PL and quantum efficiency between the $[Ru(bpy)_2L]X_2$ (**L** = L1, L2, X = Cl^-, PF_6^-, SCN^-) and $[Ru(bpy)_2(Pybm)]X_2$ (X = Cl^-, PF_6^-, SCN^-) suggest these ligands containing carrier-transporting groups are more benefit to the luminescence of the ruthenium (II) complexes than the based starting ligand (Pybm) due to the more rigid structure and more efficient shielding of the Ru (II) core towards external quenching. However, the different anions, X = Cl^-, PF_6^-, SCN^-, did not affect the emission process greatly due to the long distance between the anions and Ru core. One reversible oxidation process in the range 0.80–1.00 V exists in each of the complexes which is assigned to the metal oxidation, $[Ru(III)(bpy)_2L]^{2+} + e^- \rightleftharpoons [Ru(II)(bpy)_2L]^+$.

Acknowledgments

This work was supported by the National Natural Science Foundation of China (Grant 20971067 and 20721002), the Natural Science Foundation of Jiangsu Province (Grant BK2008257), the Major State Basic Research Development Program (2006CB806104 and 2007CB925103).

Appendix. Supporting information

Supplementary data associated with this article can be found, in the online version, at doi:10.1016/j.jorganchem.2010.04.037.

References

[1] B.S. Brunschwig, C. Creutz, N. Sutin, Coord. Chem. Rev. 177 (1998) 61–79.
[2] E.M. Kober, T.J. Meyer, Inorg. Chem. 21 (1982) 3967–3977.
[3] E.M. Kober, J.C. Marshall, W.J. Dressick, B.P. Sullivan, J.V. Caspar, T.J. Meyer, Inorg. Chem. 24 (1985) 2755–2763.

[4] T.J. Meyer, Pure Appl. Chem. 58 (1986) 1193–1206.
[5] P.A. Anderson, F.R. Keene, T.J. Meyer, J.A. Moss, G.F. Strouse, J.A. Treadway, J. Chem. Soc. Dalton Trans. (2002) 3820–3831.
[6] A.D. Guerzo, S. Leroy, F. Fages, R.H. Schmehl, Inorg. Chem. 41 (2002) 359–366.
[7] T.M. Dixon, J.P. Colin, J.P. Savage, L. Flamigini, S. Encinas, F. Barigelletti, Chem. Soc. Rev. 29 (2000) 385–391.
[8] A. Vogler, H. Kunkely, Coord. Chem. Rev. 177 (1998) 81–96.
[9] J.M. Lehn, Supramolecular Chemistry Concepts and Perspecties. VCH, New York, 1995.
[10] V. Balzani, P. Ceroni, M. Maestri, C. Saudan, V. Vicinilli, Top. Curr. Chem. 228 (2003) 159–191.
[11] V. Balzani, F. Scandola, Supramolecular Photochemistry. Horwood, Chichester U.K., 1991.
[12] G.R. Newkome, E. He, C.N. Moorefield, Chem. Rev. 99 (1999) 1689–1746.
[13] S. Serroni, S. Campagna, F. Puntoriero, C. di Pietro, N.D. McClenaghan, F. Loiseau, Chem. Soc. Rev. 30 (2001) 367–375.
[14] M. Sommovigo, G. Denti, S. Serroni, S. Campagna, C. Mingazzini, C. Mariotti, et al., Inorg. Chem. 40 (2001) 3318–3323.
[15] J.A. Barron, S. Bernhard, P.L. Houston, H.D. Abruna, J.L. Ruglovsky, G. G. Malliaras, J. Phys. Chem. A 107 (2003) 8130–8133.
[16] J.F. Callan, A.P. de Silva, N.D. McClenaghan, Chem. Commun. (2004) 2048–2049.
[17] D.C. Magri, G.J. Brown, G.D. McClean, A.P. de Silva, J. Am. Chem. Soc. 128 (2006) 4950–4951.
[18] J.D. Badijic, V. Balzani, A. Credi, S. Silvi, J.F. Stoddart, Science 303 (2004) 1845–1849.
[19] M. Gratzel, Inorg. Chem. 44 (2005) 6841–6851 (and references cited therein).
[20] M.K. Nazeeruddin (Ed.), Coord. Chem. Rev., 248, 2004, pp. 1161–1164.
[21] H.B. Baudin, J. Davidsson, S. Serroni, A. Juris, V. Balzani, S. Campagna, et al., J. Phys. Chem. A 106 (2002) 4312–4319.
[22] M. Nowakowska, V.P. Fovle, J.E. Guillet, J. Am. Chem. Soc. 115 (1993) 5975–5981.
[23] S.I. Gorelsky, E.S. Dodsworth, A.B.P. Lever, A.A. Vlcek, Coord. Chem. Rev. 174 (1998) 469–496.
[24] G. Albano, P. Belser, C. Daul, Inorg. Chem. 40 (2001) 1408–1413.
[25] J.A. Treadway, B. Loeb, R. Lopez, P.A. Anderson, F.R. Keene, T.J. Meyer, Inorg. Chem. 35 (1996) 2242–2246.
[26] A.A. Vlcek, E.S. Dodsworth, W.J. Pietro, A.B.P. Lever, Inorg. Chem. 34 (1995) 1906–1913.
[27] S. Le Gac, S. Rickling, P. Gerbaux, E. Defrancq, C. Moucheron, A. Kirsh-De Mesmaeker, Angew. Chem. Int. Ed. 48 (2009) 1122–1125.
[28] L. Moriggi, A. Aebischer, C. Cannizzo, A. Sour, A. Borel, J.C.G. Bünzli, et al., J. Chem. Soc. Dalton Trans. (2009) 2088–2095.
[29] K. Koike, S. Naito, S. Sato, Y. Tamaki, O. Ishitani, J. Photochem, Photobiol. A 207 (2009) 109–114.
[30] D.P. Rillema, D.G. Taghdiri, D.S. Jones, C.D. Keller, L.A. Worl, T.J. Meyer, et al., Inorg. Chem. 26 (1987) 578–585.
[31] K. Suzuki, A. Kobayashi, S. Kaneko, K. Takehira, T. Yoshihara, H. Ishida, et al., Phys. Chem. Chem. Phys. 42 (2009) 9850–9860.
[32] Q. Zhang, J.S. Chen, Y.X. Cheng, L.X. Wang, D.G. Ma, X.B. Jing, et al., J. Mater. Chem. 14 (2004) 895–900.
[33] Z. Peng, Z. Bao, M.E. Galvin, Adv. Mater. 10 (1998) 680–684.
[34] B.P. Sullivan, D.J. Salmon, T.J. Meyer, Inorg. Chem. 17 (1978) 3334–3341.
[35] N. Nickita, G. Gasser, P. Pearson, M.J. Belousoff, L.Y. Goh, A.M. Bond, et al., Inorg. Chem. 48 (2009) 68–81.
[36] N. Nickita, A.I. Bhatt, A.M. Bond, G.B. Deacon, G. Gasser, L. Spiccia, Inorg. Chem. 46 (2007) 8638–8651.
[37] P. Pearson, A.M. Bond, G.B. Deacon, C. Forsyth, L. Spiccia, Inorg. Chim. Acta 361 (2008) 601–612.
[38] R. Caspar, H. Amouri, M. Gruselle, C. Cordier, B. Malezieux, R. Duval, et al., Eur. J. Inorg. Chem. 3 (2003) 499–505.
[39] R. Caspar, L. Musatkina, A. Tatosyan, H. Amouri, M. Gruselle, C. Cordier, et al., Inorg. Chem. 43 (2004) 7986–7993.
[40] P. van der Sluis, A.L. Spek, Acta Crystallogr. A 46 (1990) 194–201.
[41] A. Juris, V. Balzani, F. Barigelletti, S. Campagna, P. Belser, A.V. Zelewsky, Coord. Chem. Rev. 84 (1988) 85–277.
[42] F.E. Lytle, D.M. Hercules, J. Am, Chem. Soc. 91 (1969) 253–257.
[43] M. Zhou, G.P. Robertson, J. Roovers, Inorg. Chem. 44 (2005) 8317–8325.
[44] P.A. Anderson, G.B. Deacon, K.H. Haarman, F.R. Keene, T.J. Meyer, D.A. Reitsma, et al., Inorg. Chem. 34 (1995) 6145–6157.
[45] A.E. Curtright, J.K. McCusher, J. Phys. Chem. A 103 (1999) 7032–7041.
[46] Y. Shen, B.P. Maliwal, J.R. Lakowicz, J. Fluorescence 13 (2003) 163–168.
[47] J.V. Casper, T.J. Meyer, Inorg. Chem. 22 (1983) 2444–2453.
[48] R. Alsfasser, R.V. Eldik, Inorg. Chem. 35 (1996) 628–636.
[49] B.J. Coe, T.J. Meyer, P.C. White, Inorg. Chem. 34 (1995) 593–602.
[50] K.D. Keerthi, B.K. Santra, G.K. Lahiri, Polyhedron 17 (1998) 1387–1396.
[51] S. Bhattacharya, Polyhedron 12 (1993) 235–240.
[52] S. Goswami, R.N. Mukherjee, A. Chakravorty, Inorg. Chem. 22 (1983) 2825–2832.
[53] B.K. Ghosh, A. Chakravorty, Coord. Chem. Rev. 95 (1989) 239–294.
[54] B.P. Sullivan, J.V. Caspar, S.R. Johnson, T.J. Meyer, Organometal. 3 (1984) 1241–1251.
[55] E.S. Dodsworth, A.B.P. Lever, Chem. Phys. Lett. 124 (1986) 152–158.
[56] M.A. Greaney, C.L. Coyle, M.A. Harmer, A. Jordan, E.I. Stiefel, Inorg. Chem. 28 (1989) 912–920.